THE UNIVERSITY OF
WARWICK

warwick**publications**wrap
highlight your research

http://wrap.warwick.ac.uk/

Silver antimony Ohmic contacts to moderately doped n-type germanium

D. C. S. Dumas,[1] K. Gallacher,[1] R. Millar,[1] I. MacLaren,[2] M. Myronov,[3] D. R. Leadley,[3] and D. J. Paul[1,a)]

[1]School of Engineering, University of Glasgow, Rankine Building, Oakfield Avenue, Glasgow G12 8LT, United Kingdom
[2]SUPA School of Physics and Astronomy, University of Glasgow, Kelvin Building, University Avenue, Glasgow G12 8QQ, United Kingdom
[3]Department of Physics, University of Warwick, Coventry CV4 7AL, United Kingdom

A self doping contact consisting of a silver/antimony alloy that produces an Ohmic contact to moderately doped n-type germanium (doped to a factor of four above the metal-insulator transition) has been investigated. An evaporation of a mixed alloy of Ag/Sb (99%/1%) onto n-Ge ($N_D = 1 \times 10^{18}$ cm^{-3}) annealed at 400 °C produces an Ohmic contact with a measured specific contact resistivity of $(1.1 \pm 0.2) \times 10^{-5}$ Ω-cm^2. It is proposed that the Ohmic behaviour arises from an increased doping concentration at the Ge surface due to the preferential evaporation of Sb confirmed by transmission electron microscope analysis. It is suggested that the doping concentration has increased to a level where field emission will be the dominate conduction mechanism. This was deduced from the low temperature electrical characterisation of the contact, which exhibits Ohmic behaviour down to a temperature of 6.5 K. © 2014 AIP Publishing LLC.
[http://dx.doi.org/10.1063/1.4873127]

There is an increasing interest in using Ge for both electronic and optical devices on Si substrates to expand the functionality of Si technology. Ge is an attractive material for use in many different technologies including end-of-roadmap complementary metal-oxide semiconductor (CMOS), where its higher carrier mobilities compared to Si would potentially allow for reduced power operation.[1] Ge integration has benefits for Si photonics devices[2] such as photodetectors,[3] single photon avalanche detectors,[4] modulators,[5] and Ge lasers.[6] Ge has also been used for spintronic devices[7] along with thermoelectrics[8] and there have been proposals for Ge/SiGe quantum cascade lasers.[9]

Poor electrical contacts to n-Ge are a potential roadblock to the majority of these applications. Low resistive Ohmic contacts to n-Ge are difficult to achieve because of strong Fermi level pinning at the charge neutral level (0.08–0.09 eV),[10,11] just above the valence band (Fig. 1). This produces a large Schottky barrier height at the metal-Ge interface,[12] which is relatively independent of the metal work function (pinning factor S = 0.02–0.05).[10,11] Whilst the cause of the Fermi level pinning is not fully understood, multiple methods to overcome the pinning and form an Ohmic contact have been suggested. Degenerately in-situ P doped n-Ge can support Ohmic contacts to annealed Ni.[13,14] The large dopant concentration, however, required to achieve Ohmic behaviour results in segregation of the n-type dopants during chemical vapor deposition (CVD) which is detrimental for many vertical devices since any other epitaxial layers subsequently grown will be unintentionally doped.[15] Other methods investigated include lowering the barrier height by ion implantation,[16,17] inserting an interfacial layer,[12,18–20] and the deposition of Yb capped with SiO$_2$.[21] AgSb alloys have been shown to form Ohmic contacts to low Ge

concentration n-type Si$_{1-x}$Ge$_x$ alloys,[22] leading to the investigation of AgSb for this moderately doped n-Ge layer. The method described in this paper allows a simple fabrication process to form an Ohmic contact to n-Ge doped just above the metal-insulator transition compared to alternative methods.

The n-Ge was epitaxially grown using an ASM Epsilon 2000E low pressure CVD tool on a p$^-$ Si(001) wafer.[23] The Ge layer was 2 μm thick and a phosphane precursor produced an in-situ P doping of 1×10^{18} cm^{-3}. The electrically activated dopant concentration was subsequently confirmed by Hall effect measurements on mesa etched Hall bar samples. The Mott criteria for Ge:P is 2.5×10^{17} cm^{-3} (Ref. 24) indicating that the sample is metallic with a doping level that is a factor of 4 above the metal-insulator transition.
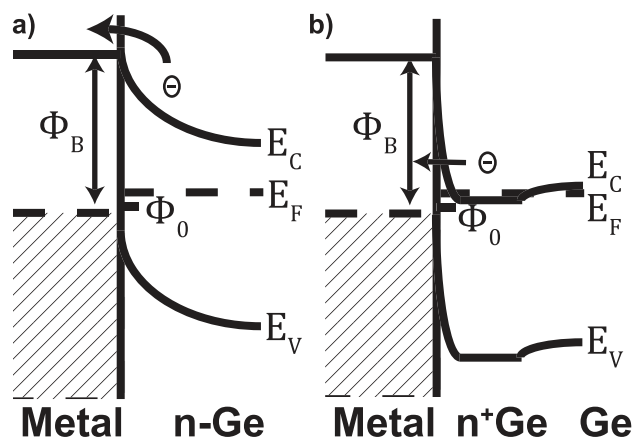
FIG. 1. A schematic diagram of a metal contact to low or moderately doped n-Ge, where the Fermi level is pinned near the charge neutral level just above the valence band. Therefore, a large Schottky barrier results, regardless of the metal work function. (b) The ideal case where the Ge is sufficiently doped to reduce the barrier width to allow tunnelling of electrons through the barrier to form an Ohmic contact.

a)Electronic mail: Douglas.Paul@glasgow.ac.uk

$15 \, mm^2$ chips for electrical measurements were prepared by first cleaning in acetone, followed by a rinse in propan-2-ol, and then blown dry in N_2. Circular transfer length method (CTLM) structures[25] were then patterned in poly(methyl methacrylate) using a Vistec VB6 electron beam lithography tool to produce devices with a placement accuracy of 1 nm. The samples were then dipped in a 5:1 buffered HF solution to remove any native oxide, before being immediately placed into a metal evaporator and pumped down to $<1 \times 10^{-6}$ millibars, where 90 nm of a mixed Ag/Sb (99%/1%) alloy was deposited by thermal evaporation. Following lift-off, the samples were annealed for 5 min in N_2 in a rapid thermal annealer at temperatures from 300–550 °C. For comparison, a reference sample was produced with 100 nm of electron-beam evaporated Ni and annealed at 340 °C for 30 s which produces a germanide phase (NiGe) that has the lowest resistivity out of all the transition metals.[13,14,26–29] It is therefore often used to make a contact to n-Ge and to date has resulted in the lowest values of specific contact resistivity (ρ_c).[14] This approach, however, requires highly doped Ge ($N_D > 1 \times 10^{19} \, cm^{-3}$), where conduction is dominated by field emission through a thin Schottky barrier. Therefore, for lower doped n-Ge such as the material investigated in this work, it is anticipated that a Schottky contact will form because conduction will be reliant on thermionic emission over the barrier (Fig. 1).

Each chip contained multiple CTLM structures with inner radii ranging from 50 to $100 \, \mu m$, which are more than a few times the transfer length[25] (around $7.5 \, \mu m$) and gap spacings ranging from $2 \, \mu m$ to $100 \, \mu m$, comparable to others,[27] the outer contact was contained within an $800 \, \mu m \times 800 \, \mu m$ square. The CTLM structures were characterised using a four connections (separate force and sense for voltage and current) dc configuration with a voltage sweep from -2 to 2 V using an Agilent B1500 semiconductor parameter analyser. Unlike linear TLM structures the CTLMs can be fabricated in a single lithography step since they do not require a mesa etch to confine the current path. Therefore, this removes errors related to lithographic misalignment between the mesa etch and contact deposition. The total resistance of each structure is measured and then plotted as a function of the gap spacing. A geometric correction factor[25] is required such that the resistance divided by the correction factor is a linear function of the gap spacing, which allows a linear fit to the data (Fig. 2). From this, the sheet resistance (R_{sh}) and the transfer length (L_T) can be extracted. The ρ_c is then calculated by using[25] $\rho_c = L_T^2 \times R_{sh}$.

Figure 3 shows the current-voltage (IV) characteristics of $50 \, \mu m$ radius CTLM structures with $100 \, \mu m$ gap spacing for the AgSb contacts annealed at 300–550 °C for 5 min. For comparison, the NiGe contact is also plotted. It is obvious that the AgSb contacts annealed at 300 °C and 350 °C both demonstrate Schottky behaviour. Both show better current conduction, however, compared to the NiGe contact, implying that some of the Sb has been activated by the anneal. The contacts annealed at 400 °C and 450 °C are clearly Ohmic (Fig. 3), as characterised by the symmetry and high current density for the forward and reverse biases. This suggests that more Sb has become electrically active and the n-Ge dopant concentration has increased to a level where field emission dominates conduction. Anneal temperatures higher than
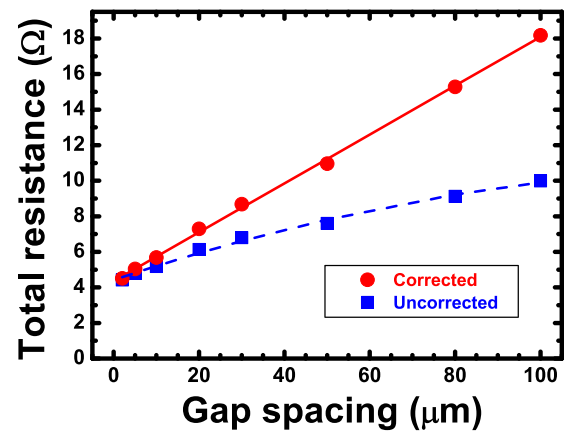

FIG. 2. The measured and corrected resistance values for a Ag/Sb (99%/1%) alloy on n-Ge CTLM structure with $50 \, \mu m$ radius annealed at 400 °C with a linear fit applied to the corrected values.
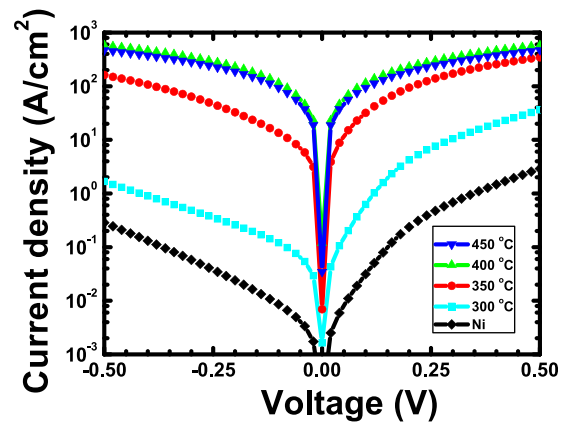

FIG. 3. The semi-log current density versus voltage characteristics for a 90 nm 99% Ag/1% Sb alloy on n-Ge annealed at 300–550 °C. The NiGe sample annealed at 340 °C is also shown (black line). The AgSb on n-Ge contacts annealed at 400 and 450 °C for 5 min are clearly Ohmic.

450 °C resulted in agglomeration of the contact, which is evident in the atomic force microscopy image in Fig. 4.

Since the AgSb contacts annealed at 400 °C and 450 °C were Ohmic, the ρ_c was extracted from the CTLM structures and are summarised in Table I. The best result was obtained for a AgSb alloy on n-Ge contact annealed at 400 °C for
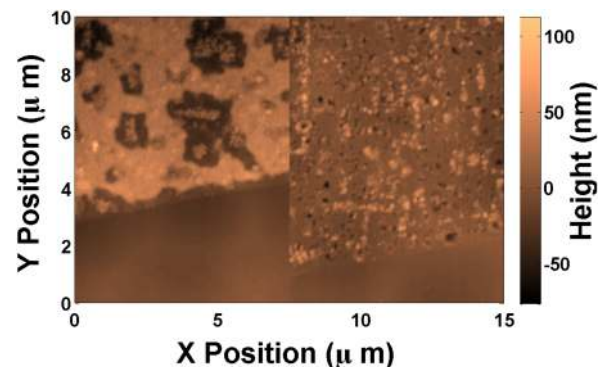

FIG. 4. Surface roughness map of the AgSb on n-Ge contact annealed at 500 °C (left) and 550 °C (right) measured with an atomic force microscope. The smooth surface in the bottom of the figure corresponds to an area of blank Ge.

TABLE I. The contact type that arises for a AgSb alloy on n-Ge annealed at different temperatures. The specific contact resistivity is included for the Ohmic contacts.

Anneal (°C)	Contact	ρ_c (Ω-cm^2)
≤ 350	Schottky	…
400	Ohmic	$(1.1 \pm 0.2) \times 10^{-5}$
450	Ohmic	$(1.7 \pm 0.3) \times 10^{-5}$
≥ 500	Agglomerated	…

5 min. The contact was shown to be stable up to an anneal time of 10 min. The IV characteristics of the contact was measured as a function of sample temperature and this is shown in Fig. 5. It is clear that the contact remains Ohmic down to the base temperature of the measurement cryostat of 6.5 K. There is noticeable improvement in the current conduction for the IVs at 6.5 K and 77 K compared to room temperature, which can be explained from an increase in conductivity for the as grown n-Ge at lower temperatures.[30] The Ohmic behaviour at 77 K and below is another indication that field emission is the dominant conduction mechanism. Therefore, this implies that the doping concentration of the n-Ge under the contact has been increased due to the Sb evaporation and subsequently electrically activated from the anneal. Since the solid solubility limit of Sb in Ge is 5 orders of magnitude higher than Ag at these anneal temperatures[31] enhanced Sb doping at the metal/Ge interface is expected. To highlight the performance of this contact further, the IV characteristics for the NiGe contact at room temperature are plotted in Fig. 5 and is clearly rectifying.

Since the NiGe contact is rectifying, due to Fermi level pinning, the Schottky barrier height (ϕ_B) can be calculated by[32]

$$\phi_B = \frac{k_B T}{q} \ln\left(\frac{AA^* T^2}{I_S}\right), \qquad (1)$$

where k_B is the Boltzmann constant, T is the temperature in K, A is the area of the contact, and A^* is 143 A cm^{-2} K^{-2} for Ge (Ref. 11). I_S is the saturation current, which is equal to the y-intercept of a linear fit to $\log_{10}\left(I/(1 - e^{-qV/k_B T})\right)$
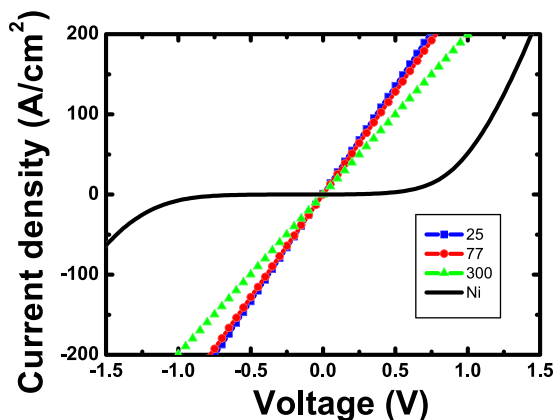

FIG. 5. The current density versus voltage characteristics measured at different temperatures for a 90 nm AgSb alloy on n-Ge contact annealed at 400 °C for 5 min. For comparison, the room temperature IV for the NiGe contact annealed at 340 °C is displayed (black line).

versus voltage for the contact in forward bias near zero volts.[32] From the IV characteristics of a sample with a large AgSb Ohmic contact and 140 μm $\times$ 140 μm NiGe contact a barrier height of 523 $\pm$ 11 meV and an ideality factor of 1.20 was extracted from the slope of the linear fit, which is consistent with values previously measured.[10,11,33] Due to the large barrier height and low doping concentration (1×10^{18} cm^{-3}) the NiGe contact is reliant on thermionic emission over the barrier (Fig. 1). This shows the advantage of this AgSb process, which is self-doping, in creating an Ohmic contact to moderately doped n-Ge by increasing the dopant concentration.

To investigate the AgSb contact annealed at 400 °C in more detail, the contact was analysed using scanning transmission electron microscopy (STEM). Samples were prepared by the focused ion beam (FIB) lift-out process using a FEI Nova Nanolab 200 Dualbeam FIB microscope. STEM characterisation was then performed on the resulting sections using a JEOL ARM200F microscope equipped with a cold field emission gun electron source and a Gatan GIF Quantum electron energy loss spectrometer. Characterisation was performed using electrons accelerated to 200 kV, with images recorded using the high-angle annular dark-field (HAADF) mode and dual electron energy loss spectrum (DualEELS) images recorded over an energy range up to 2100 eV covering the edges for Ag M$_{4,5}$, Sb M$_{4,5}$, and Ge L$_{2,3}$, as well as C K. Quantification was performed using a new convolution-based approach provided by Gatan Inc. (Pleasanton, USA) based on earlier work by Verbeeck *et al.*[34,35] which fits the fine structure at the absorption edges based on the low loss spectrum and thus accounts for multiple scattering explicitly through the use of the whole DualEELS dataset. The HAADF image of Fig. 6 shows a cross-section of a contact annealed at 400 °C for 5 min. The distribution of the Ag, Sb, and Ge are shown both separately and as a multicoloured overlay map. In both the image and the maps, it is clear that, unlike Ni$_x$Ge$_y$ contacts,[13] the AgSb forms a predominately flat contact on the surface, with just the occasional dip into the Ge. It is also observed that the Sb has diffused to a depth of $\approx$5 nm at a concentration of a few percent. This is significant enough to increase the dopant concentration of n-Ge. The top surface of the contact is rougher. This is most likely due to the fact that the contact is polycrystalline with nanosized grains. The estimates from our DualEELS quantification suggest an approximate 75% Ag/25% Sb composition confirming that Sb is preferentially evaporated from the target, enriching it significantly in the film. This may also suggest that the composition
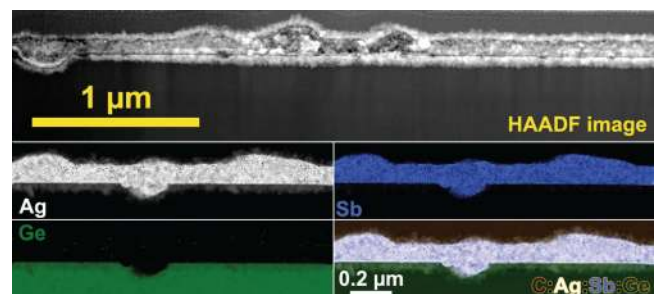

FIG. 6. HAADF images of a AgSb on n-Ge contact annealed at 400 °C for 5 min.

would be graded in a thicker Ag contact through depletion of the Sb in the target.

To conclude, to reduce n-type dopant segregation during epitaxial growth, n-Ge Ohmic contact layers grown below nominally undoped active layers require lower doping concentrations than that required to produce low ρ_c Ohmic contacts. The NiGe Ohmic contacts to n-Ge requires a highly doped layer ($N_D > 1 \times 10^{19}$ cm^{-3}), otherwise a Schottky contact forms. Other processes that have been demonstrated require additional steps, adding to the complexity of the contact scheme. A process for the creation of Ohmic contacts to n-Ge ($N_D = 1 \times 10^{18}$ cm^{-3}), which requires only a AgSb alloy deposition and an anneal has been demonstrated. A deposition of a AgSb alloy followed by a $400\,^\circ$C anneal for 5 min can produce an Ohmic contact with a ρ_c of $(1.1\pm0.2) \times 10^{-5}$ Ω-cm^2 on n-Ge layers doped to a factor of four above the metal insulator transition. The contacts remained Ohmic down to 6.5 K indicating that field emission is the main electrical conduction mechanism.

[1]R. Pillarisetty, Nature **479**, 324 (2011).

[2]D. J. Paul, Electron. Lett. **45**, 582 (2009).

[3]S. J. Koester, J. D. Schaub, G. Dehlinger, and J. O. Chu, IEEE J. Sel. Top. Quantum Electron. **12**, 1489 (2006).

[4]R. E. Warburton, G. Intermite, M. Myronov, P. Allred, D. R. Leadley, K. Gallacher, D. J. Paul, N. J. Pilgrim, L. J. M. Lever, Z. Ikonic, R. W. Kelsall, E. Huante-Ceron, A. P. Knights, and G. S. Buller, IEEE Trans. Electron Devices **60**, 3807 (2013).

[5]Y. H. Kuo, Y. K. Lee, Y. S. Ge, S. Ren, J. E. Roth, T. I. Kamins, D. A. B. Miller, and J. S. Harris, Nature **437**, 1334 (2005).

[6]R. E. Camacho-Aguilera, Y. Cai, N. Patel, J. T. Bessette, M. Romagnoli, L. C. Kimerling, and J. Michel, Opt. Express **20**, 11316 (2012).

[7]C. Shen, T. Trypiniotis, K. Y. Lee, S. N. Holmes, R. Mansell, M. Husain, V. Shah, X. V. Li, H. Kurebayashi, I. Farrer, C. H. de Groot, D. R. Leadley, G. Bell, E. H. C. Parker, T. E. Whall, D. A. Ritchie, and C. H. W. Barnes, Appl. Phys. Lett. **97**, 162104 (2010).

[8]L. F. Llin, A. Samarelli, S. Cecchi, T. Etzelstorfer, E. M. Gubler, D. Chrastina, G. Isella, J. Stangl, J. M. R. Weaver, P. S. Dobson, and D. J. Paul, Appl. Phys. Lett. **103**, 143507 (2013).

[9]D. J. Paul, Laser Photonics Rev. **4**, 610 (2010).

[10]A. Dimoulas, P. Tsipas, A. Sotiropoulos, and E. K. Evangelou, Appl. Phys. Lett. **89**, 252110 (2006).

[11]T. Nishimura, K. Kita, and A. Toriumi, Appl. Phys. Lett. **91**, 123123 (2007).

[12]Y. Zhou, M. Ogawa, X. Han, and K. L. Wang, Appl. Phys. Lett. **93**, 202105 (2008).

[13]K. Gallacher, P. Velha, D. J. Paul, I. MacLaren, M. Myronov, and D. R. Leadley, Appl. Phys. Lett. **100**, 022113 (2012).

[14]K. F. Gallacher, P. Velha, D. J. Paul, I. Maclaren, M. Myronov, and D. R. Leadley, ECS Trans. **50**, 1081 (2013).

[15]J. Hartmann, V. Loup, G. Rolland, P. Holliger, F. Laugier, C. Vannuffel, and M. Semeria, J. Cryst. Growth **236**, 10 (2002).

[16]M. Koike, Y. Kamata, T. Ino, D. Hagishima, K. Tatsumura, M. Koyama, and A. Nishiyama, J. Appl. Phys. **104**, 023523 (2008).

[17]G. Thareja, S. L. Cheng, T. Kamins, K. Saraswat, and Y. Nishi, IEEE Electron Device Lett. **32**, 608 (2011).

[18]Z. Li, X. An, M. Li, Q. Yun, M. Lin, M. Li, X. Zhang, and R. Huang, IEEE Electron Device Lett. **33**, 1687 (2012).

[19]J. -Y. J. Lin, A. M. Roy, A. Nainani, Y. Sun, and K. C. Saraswat, Appl. Phys. Lett. **98**, 092113 (2011).

[20]P. Paramahans Manik, R. Kesh Mishra, V. Pavan Kishore, P. Ray, A. Nainani, Y.-C. Huang, M. C. Abraham, U. Ganguly, and S. Lodha, Appl. Phys. Lett. **101**, 182105 (2012).

[21]Z.-W. Zheng, T.-C. Ku, M. Liu, and A. Chin, Appl. Phys. Lett. **101**, 223501 (2012).

[22]S. F. Nelson and T. N. Jackson, Appl. Phys. Lett. **69**, 3563 (1996).

[23]V. A. Shah, A. Dobbie, M. Myronov, and D. R. Leadley, Solid-State Electron. **62**, 189 (2011).

[24]P. P. Edwards and M. J. Sienko, Phys. Rev. B **17**, 2575 (1978).

[25]J. Klootwijk and C. Timmering, in *Proceedings of the IEEE International Conference on Microelectonics Test Structures* (2004), pp. 247–252.

[26]S. Gaudet, C. Detavernier, A. Kellock, P. Desjardins, and C. Lavoie, J. Vac. Sci. Technol., A **24**, 474 (2006).

[27]A. Firrincieli, K. Martens, R. Rooyackers, B. Vincent, E. Rosseel, E. Simoen, J. Geypen, H. Bender, C. Claeys, and J. A. Kittl, Appl. Phys. Lett. **99**, 242104 (2011).

[28]K. Ikeda, Y. Yamashita, N. Sugiyama, N. Taoka, and S.-i. Takagi, Appl. Phys. Lett. **88**, 152115 (2006).

[29]M. Shayesteh, K. Huet, I. Toque-Tresonne, R. Negru, C. L. M. Daunt, N. Kelly, D. O'Connell, R. Yu, V. Djara, P. B. Carolan, N. Petkov, and R. Duffy, IEEE Trans. Electron Devices **60**, 2178 (2013).

[30]C. S. Hung and J. R. Gliessman, Phys. Rev. **96**, 1226 (1954).

[31]F. Trumbore, Bell Systems Tech. J. **39**, 205 (1960).

[32]D. Schroder, *Semiconductor Material and Device Characterization* (IEEE Press, 2006).

[33]H. Yao, C. Tan, S. Liew, C. Chua, C. Chua, R. Li, R. Lee, S. Lee, and D. Chi, in *Proceedings of the International Workshop on Junction Technology* (2006), pp. 164–169.

[34]J. Verbeeck and S. Van Aert, Ultramicroscopy **101**, 207 (2004).

[35]J. Verbeeck, S. Van Aert, and G. Bertoni, Ultramicroscopy **106**, 976 (2006).